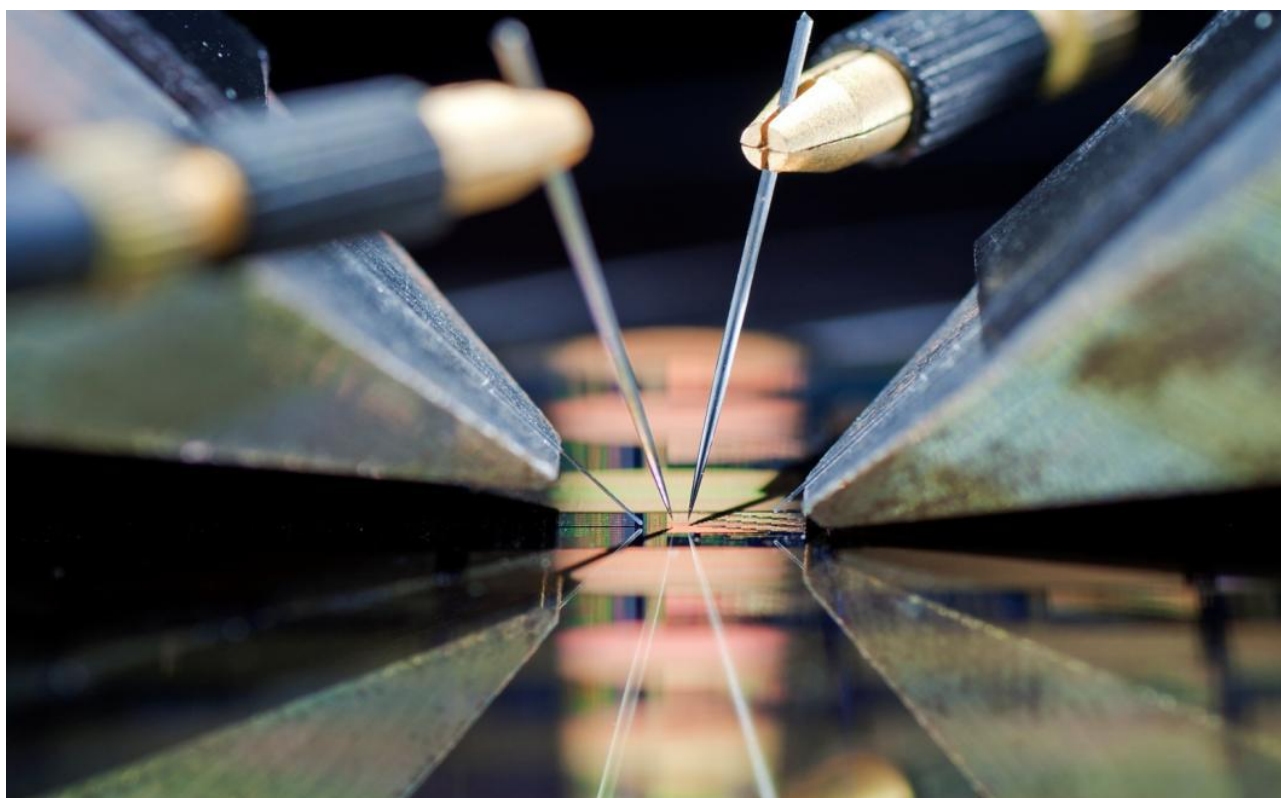




UNIVERSITY  
OF TRENTO - Italy  
Department of Physics



# NANOSCIENCE LABORATORY



## HIGHLIGHTS 2011

## NANOSCIENCE LABORATORY HIGHLIGHTS 2011

### MEMBERS (2011)

#### Faculty and research staff

Lorenzo Pavesi (full professor, director)  
Marina Scarpa (full professor)  
Zeno Gaburro (assistant professor)

#### Technical staff

Massimo Cazzanelli (EP2 level)  
Paolo Bettotti (EP1 level)  
Elvira Damato (left 5.2011)  
Enrico Moser

#### Administrative staff

Tatsiana Yatskevich

#### Post-doctoral fellows

Nicola Daldosso (left 5.2011)  
Oleksiy Anopchenko  
Elena Froner  
Silvia Larcheri  
Philip Ingenhoven (from 1.2011)  
Bing Han (left 4.2011)

Romain Guider (left 1.2011)  
Benjamin Dierre (left 1.2011)  
Kamil Fedus  
Fernando Ramiro Manzano  
Francisco Aparicio Rebollo

#### Doctoral students

Marco Masi (thesis 2.2011)  
Alessandro Marconi (thesis 11.2011)  
Nikola Prtljaga  
Eveline Rigo (Università di Modena)  
Mattia Mancinelli  
Federica Bianco  
Fabrizio Sgrignuoli  
Andrea Tengattini  
Neeraj Kumar  
Davide Gandolfi

#### Master students

Alberto Battarelli

### SCIENTIFIC MISSION

#### Introduction to the Nanoscience Laboratory

The Nanoscience Laboratory (NL) is a laboratory of the Physics Department with interests in nanophotonics, silicon-based photonics and nanobiotechnologies. Its mission is to generate new knowledge and understanding from physical phenomena which occur when the matter is of nanometer size. In particular, NL is trying to apply the nanoscience paradigm to silicon or silicon compatible materials to enable new application of this key material, and to develop nanosystems compatible with the main driving silicon technologies. However silicon is not the only material studied. New projects concern the use of polymers to tailor the properties of nanostructure atom-by-atom or metals to investigate new properties which rise from plasmonics.

A particular emphasis is placed on photonics and its applications. Research projects span from fundamental research work on the interaction between biomolecules and silicon nanostructures or on the control of photons by dynamically structuring the dielectric environment, to more applied research work on the development of integrated optical circuits, optical switches, light emitting devices and amplifiers, novel MIR and THz sources, third generation photovoltaic and biosensors.

NL is composed by more than 20 people with interdisciplinary

scientific background. Researchers from physics, bio-chemistry, materials science and electrical engineering interact to form a group of interdisciplinary nature. They came from all around the world and the language spoken in the laboratory is English.

Of particular mention is the collaboration that NL has with the Center of Materials and Microsystems, in particular with the Advance Photonics and Photovoltaic and the Biofunctional Surfaces and Interfaces units, of the Fondazione Bruno Kessler (FBK). The collaboration spans over the last twenty years and covers fabrication, testing and application of biomaterials and silicon based devices. Many common projects exist among which a project on the development of a multispectral protein chip for application in diagnostics (NAOMI, supported by Provincia Autonoma di Trento (PAT)).

NL, with the help of the local institutes of CNR and FBK, organizes each two years a winter school on optoelectronics and photonics: the 6<sup>th</sup> Photonics and Optoelectronics Winter School: Physics and Application of T-Rays, was held at the end of February 2011. Members of NL participate in the committee or organize several international conferences or workshop.

Research of NL is mainly funded by the local government (PAT), the European commission within the research frameworks, the MIUR and by companies. During the period covered by these Highlights, NL has been and is involved in the following projects: NAOMI (supported by PAT), project on the development of a MIR micro source (supported by the foundation CARIPLO), collaborative project Italy-Spain, Italy-Turkey and Italy-India

(ITPAR) supported by the Ministry of Education, University and Research, some European projects within the 7<sup>th</sup> Framework: WADIMOS (FP7-ICT-216405), HELIOS (FP7-ICT-224312), LIMA (FP7-ICT-248909), POSITIVE (FP7-ICT-257401), El-Dorado (FP7-PEOPLE-235860), APPCOPTOR (FP7-PEOPLE-275150).

### Silicon Nanophotonics

Silicon photonics is the technology where photonic devices are produced by standard microelectronic processes using the same paradigm of electronics: integration of a large number of devices to yield a high circuit complexity which allows for high performances and low costs. Here, the real truth is to develop photonic devices that can be easily integrated to improve the single device performance and to allow high volume production.

We are involved in researching new optical scheme for implementing optical network on a chip by using concepts of nanophotonics. Transport phenomena of charge carriers in solids have several analogies with the propagation of light waves in dielectric materials. Electronic crystals have an analogue in the form of photonic crystals which are artificial materials, where a periodic variation of dielectric constant leads to the formation of bands where the propagation of photons is allowed or forbidden. In the past years we have developed one dimensional complex dielectric systems based on porous silicon multilayers with the aim of studying in depth the photon propagations in these complex systems. Nowadays, we use the concept of whispering gallery modes which develops in micro-disks or micro-rings to further tune the photon mode density. These disks or rings are coupled directly with narrow mode SOI (Silicon-on-Insulator) waveguides. High quality factor cavities allow to study fundamental quantum optics concept such as Purcell effects or optical forces. Series of coupled micro-rings are studied to implement novel scheme of phase controlled optical networks where EIT (electromagnetic induced transparency) is manifested and exploited to route optical signals.

To develop silicon photonics, one further add-on is making silicon do something which it is not able to do in its standard (bulk) form. Low dimensional silicon, where small silicon nanocrystals or nanoclusters (Si-nc) are developed, is one way to compel silicon to act as an active optical material. The key ingredient that makes Si-nc appealing for photonics are: quantum size effects which makes new phenomena appear in silicon, such as room temperature visible photoluminescence, optical gain, coulomb blockade and multiexciton generation. Our research interests are to exploit quantum confinement and reduced dimensionality to produce effective light sources, lasers, optical amplifiers. In addition, we use quantum confinement to increase the nonlinear optical properties of silicon and to achieve optical switching. Finally, two new activities which are being developed concern the use of strain to tune the nonlinear optical properties of silicon waveguides and the fabrication of polymer devices on silicon to implement polymer-on-silicon photonics.

### Nanobiotechnologies, antioxidants and human health

All the aspects related to the nano-bio interfaces (which are the structures where the co-existence of physical principles and biological molecules is clearly evident) are a challenging field of research. Though the leading research concerns the design, synthesis and dynamic behavior of nano-structured bio-interfaces, more specifically we are working on three research topics: silicon- and titanium based nanosystems, single molecule detection, and anti-

oxidant behavior in micelle systems.

To develop silicon based bio-sensors, we are currently focused on silicon based hybrid nanostructures. In particular silicon or silicon nitride flat or porous films are the starting inorganic support into which bio active layers are designed. Biological recognition elements are introduced on this hybrid layer. Molecular surface density, active layer thickness and integration of the bio-active interface with photonic devices will be the future challenges to develop the sensor system. In addition, we are developing nanostructured hybrid interfaces to capture bio-analytes and enhance their Raman signals. Gold and silver nanoparticles are used as enhancers.

Beyond traditional sensor applications, silicon nanostructures can be used as “nanosensors”, which monitor the intracellular events without introducing irreversible perturbations. To this regard light emitting silicon quantum dots appear very promising. We are studying the nanoparticle coating to increase optical stability and decrease toxicity, moreover conjugation to biological molecules and strategies to increase cell uptake and control intracellular localization are future steps of this research. Titanium nanotubes showing hydroxyl-rich interfaces have been synthesized. These nanosystems are easily dispersed and stable in aqueous solutions and show a high photocatalytic activity.

Antioxidant compounds are able to control reactive and damaging forms of oxygen, referred to as free radicals. Though antioxidants have been largely studied, much remains unknown about the human body adsorption and use of these compounds. We are investigating the synergistic effect of plasma antioxidants at the interface of micelle systems. Beyond the basic biophysical investigation, the crucial point is the development of devices and methodologies to monitor the antioxidant action. Being these processes free-radical mediated, a very high detection sensitivity is required. Moreover, to have physiological significance, the experiments should be performed in heterogeneous systems mimicking an unperturbed biological environment. Thus we are proposing a new theoretically based methodology to compute antioxidant capacity and efficiency starting from oxygen concentration measurement, as well as, we are designing a nanostructured electrode to monitor molecular oxygen in real time.

### Experimental facilities

The NL facilities allow for detailed experimental studies in nanoscience, photonics and biotechnologies. Since the effective collaboration with FBK most material processing and device productions are performed within their premises.

For photonics, we have facilities to cover the light spectrum from the THz to UV ranges with whatever time resolution is needed. Laser sources comprehends: Ti-sapphire fs-ps laser (1 W average over 1000-700 nm, 2 ps or 70 fs pulses, 82 MHz repetition rate) interfaced with a second harmonic generator and pulse picker; Nd-Yag laser interfaced with an optical parametric oscillator which allows scanning the 400-3000 nm wavelength region (pulse 50 mJ, 10 ns, 10 Hz); TOPAS pumped with an amplified Ti:Sa laser which covers the 1-2.6  $\mu\text{m}$  range with 35 fs, 10 kHz, 3 mJ; one CW, UV extendend, Ar laser; two fiber pig-tailed tunable CW lasers (1200 - 1700 nm and 1500 - 1600nm); several pig-tailed diode lasers, ASE source at 1550 nm, a power amplifier to more than 1W at 1550 nm and a broad band SLD at 800 nm. Three high-power true-CW DPSS single-line laser operating at 532, 473 and 355 nm. Detectors comprehend: visible and infrared photomultipliers and CCDs, a streak camera with ps resolution, 4K cooled bolometers which cover THz region, avalanche photodi-

odes for vis and IR ranges plus one capable of photon-counting in the third telecom window. To perform spectral analysis several set-ups are available: FTIR and dispersive spectrophotometers, a micro-Raman setup, a micro-FTIR and a UV-vis-IR spectrophotometer (shared with other laboratories), UV-Vis and fluorescence spectrophotometer dedicated to biochemical experiments. Five dedicated apparatus for WG characterization equipped with nanopositioning systems and polarization controllers are available, each one specified on a given functions: visible, infrared, pump-probe, grating coupling and non-linear measurements. Other apparatus are: - visible and infrared photoconductivity set-up; - a solar simulator for cell sizes up to 5 inches; - two nanoprobe stations (AFM and SNOM) coupled with a femto-jet system for local infiltration of the samples and biological experiments; - two semiconductor electrical-optical probe stations (4 and 8 inches) and many different electrical characterization set-ups (I-V, Z- $\omega$ , EL-I, etc.). Two VIS to NIR optical spectrum analyzers are available to NL-Lab. A probe station is fiber-bunch interfaced with a spectrometer interfaced with IR and visible liquid nitrogen cooled CCD. For sample production and treatment and high sensitivity analytical detection, an electrochemical laboratory equipped with several chemical hots, spinners, galvanostates and voltameters is available. An electron beam lithography set-up (SEM attachment) is also owned. For optical, electrical molecular dynamic simulations, the laboratory uses free and commercial software, a dedicated cluster with 16 nodes and work-stations. Two laboratories one dedicated to chemical synthesis and the second to biological sample preparation are also available.

## 2011 publications

1. "Electroluminescence from Si nanocrystal/c-Si heterojunction light-emitting diodes", D. Di, I. Perez-Wurfl, L. Wu, Y. Huang, A. Marconi, A. Tengattini, A. Anopchenko, L. Pavesi, G. Conibeer, *Appl. Phys. Lett.*, 99, 251113 (2011)
2. "Continuous wave spectroscopy of nonlinear dynamics of Si nanocrystals in a microdisk resonator", M. Xie, A. Pitanti, M. Ghulinyan, D. Yang, G. Pucker, L. Pavesi, *Phys. Rev. B*, 84, 245312 (2011)
3. "Copropagating pump and probe experiments on Si-nc in SiO<sub>2</sub> rib waveguides doped with Er: The optical role of non-emitting ions", D. Navarro-Urrios, F. Ferrarese Lupi, N. Prtljaga, A. Pitanti, O. Jambois, J. M. Ramirez, Y. Berencen, N. Daldosso, B. Garrido, L. Pavesi, *Appl. Phys. Lett.*, 99, 231114 (2011)
4. "Birefringent porous silicon membranes for optical sensing", J. Alvarez, P. Bettotti, I. Suarez, N. Kumar, D. Hill, V. Chirvony, L. Pavesi, J. Martinez-Pastor, *Opt. Express*, 19, 26106 (2011)
5. "Graded-size Si quantum dot ensembles for efficient light-emitting diodes", A. Anopchenko, A. Marconi, M. Wang, G. Pucker, P. Bellutti, L. Pavesi, *Appl. Phys. Lett.*, 99, 181108 (2011)
6. "Light propagation with phase discontinuities: generalized law of reflection and refraction", N. Yu, P. Genevet, M. A. Kats, F. Aieta, J.-P. Tetienne, F. Capasso, Z. Gaburro, *Science*, 334, 333 (2011)
7. "Effect of radiation damping on the spectral response of plasmonic components", M. A. Kats, N. Yu, P. Genevet, Z. Gaburro, F. Capasso, *Opt. Express*, 19, 21748 (2011)
8. "Silicon nanocrystal light emitting device as a bidirectional optical transceiver", A. Marconi, A. Anopchenko, G. Pucker, L. Pavesi, *Semicond. Sci. Technol.*, 26, 095019 (2011)
9. "On-chip silicon-based active photonic molecules by complete photonic bandgap light confinement", B. Qian, K. Chen, S. Chen, W. Li, X. Zhang, J. Xu, X. Huang, L. Pavesi, C. Jiang, *Appl. Phys. Lett.*, 99, 034105 (2011)
10. "Electroluminescence and charge storage characteristics of quantum confined germanium nanocrystals", S. Das, R. K. Singha, A. Dhar, S. K. Ray, A. Anopchenko, N. Daldosso, L. Pavesi, *J. Appl. Phys.*, 110, 024310 (2011)
11. "Optical characterization of silicon-on-insulator based single and coupled racetrack resonators", M. Mancinelli, R. Guider, P. Bettotti, M. Masi, M. R. Vanacharla, J.-M. Fedeli, D. Van Thourhout, L. Pavesi, *J. Nanophotonics*, 5, 051705 (2011)
12. "A silicon photonic interferometric router device based on SCISSOR concept", M. Masi, M. Mancinelli, M. R. Vanacharla, A. Battarelli, R. Guider, P. Bettotti, J.-M. Fedeli, L. Pavesi, *J. Lightwave Technol.*, 29, 2747 (2011)
13. "Optical characterization of a SCISSOR device", M. Mancinelli, R. Guider, M. Masi, P. Bettotti, M. R. Vanacharla, J.-M. Fedeli, L. Pavesi, *Opt. Express*, 19, 13664 (2011)
14. "Monolithic Whispering-Gallery Mode Resonators With Vertically Coupled Integrated Bus Waveguides", M. Ghulinyan, R. Guider, G. Pucker, L. Pavesi, *IEEE Photonic Tech. L.*, 23, 1166 (2011)
15. "Modeling of Slot Waveguide Sensors Based on Polymeric Materials", P. Bettotti, A. Pitanti, E. Rigo, F. De Leonardis, V. M. N. Passaro, L. Pavesi, *Sensors*, 11, 7327 (2011)
16. "Coupled-resonator-induced-transparency concept for wavelength router applications", M. Mancinelli, R. Guider, P. Bettotti, M. Masi, M. R. Vanacharla, L. Pavesi, *Opt. Express*, 19, 12227 (2011)
17. "Si nanoclusters coupled to Er<sup>3+</sup> ions in a SiO<sub>2</sub> matrix for optical amplifiers", D. Navarro-Urrios, O. Jambois, F. Ferrarese Lupi, P. Pellegrino, B. Garrido, A. Pitanti, N. Prtljaga, N. Daldosso, L. Pavesi, *Opt. Mater.*, 33, 1086 (2011)
18. "Power efficiency estimation of silicon nanocrystals based light emitting device in alternating current regime", A. Marconi, A. Anopchenko, G. Pucker, L. Pavesi, *Appl. Phys. Lett.*, 98, 201103 (2011)
19. "Efficiency and capacity of antioxidant rich foods in trapping peroxy radicals: A full evaluation of radical scavenging activity", P. Vanzani, M. Rossetto, V. De Marco, A. Rigo, M. Scarpa, *Food research international* 44, 269 (2011)
20. "Active site residue involvement in monoamine or diamine oxidation catalysed by pea seedling amine oxidase", M.L. Di Paolo, M. Lunelli, M. Fuxreiter, A. Rigo, I. Simon, M. Scarpa, *FEBS Journal* 278, 1232 (2011)
21. "Erbium implanted silicon rich oxide thin films suitable for slot waveguides applications", N. Prtljaga, D. Navarro-Urrios, A. Marconi, A. Anopchenko, J.-P. Colonna, F. Milesi, N. Daldosso, O. Jambois, B. Garrido, J.-M. Fedeli, and L. Pavesi, *Opt. Mater.*, 33, 1083-1085 (2011).
22. "Light emission and floating gate memory characteristics of germanium nanocrystals", S. Das, S. Manna, R. Singha, A. Anopchenko, N. Daldosso, L. Pavesi, A. Dhar, S. K. Ray, *Phys. Status Solidi A*, 208, 635 (2011).



23. "Photoluminescence of hydrophilic silicon nanocrystals in aqueous solutions", N. Prtljaga, E. D'Amato, A. Pitanti, R. Guider, E. Froner, S. Larcheri, M. Scarpa, L. Pavesi, *Nanotechnology*, 22, 215704 (2011).
24. "Deoxycholate as an efficient coating agent for hydrophilic silicon nanocrystals", E. Froner, E. D'Amato, R. Adamo, N. Prtljaga, S. Larcheri, L. Pavesi, A. Rigo, C. Potrich, M. Scarpa, *J. Colloid Interf. Sci.*, 358, 86 (2011).
25. "Robust design of an optical router based on tapered side coupled integrated spaced sequence of optical resonators", P. Bettotti, M. Mancinelli, R. Guider, M. Masi, M. Rao Vannacharla, L. Pavesi, *Opt. Lett.*, 36, 1473 (2011).
26. "Broad-band tunable visible emission of sol-gel derived Si-BOC ceramic thin films", A. Karakuscu, R. Guider, L. Pavesi, G. D. Sorarù, *Thin Solid Film*, 519, 3822 (2011).
27. "Silicon nanocrystals as a photoluminescence down shifter for solar cells", Z. Yuan, G. Pucker, A. Marconi, F. Sgrignuoli, A. Anopchenko, Y. Jestin, L. Ferrario, P. Bellutti, L. Pavesi, *Sol. Energy Mater. Sol. Cells*, 95, 1224 (2011).
28. "Nanosilicon: a new platform for photonics", P. Bettotti, L. Pavesi, *Phys. Stat. Sol. (c)*, 8, 2880 (2011).
29. "Role of kinetic energy of impinging molecules in the  $\alpha$ -sexithiophene growth", M. Tonezzer, E. Rigo, T. Toccoli, S. Gottardi, P. Bettotti, L. Pavesi, S. Iannotta, *Thin Solid Films*, 519, 4110 (2011).

## 1. Nanocrystalline silicon and silver Nanoparticles in photovoltaics (Philip Ingenhoven)

Silicon nanocrystals (Si-nc) in silicon oxide (fig. 1) are a potentially interesting material for photovoltaic devices due to their photoluminescence properties. Quantum confinement of excitons in Si-nc yields the possibility to tune at will the band gap which, in turn, is wider than the one of bulk Si. In silicon solar cells, the solar power conversion efficiency is severely limited by the thermalization of hot carriers which are excited at high energy and thermalize to the silicon band gap. Si-nc can be used as optical downshifter layer coating the surface of standard silicon cells. In fact, Si-nc absorb high energy photons that are poorly converted to electrical energy in the solar cell and emit low energy photons which are re-absorbed by the cell and efficiently converted into electricity. We are currently exploring the possibility to enhance this effect with the help of a layer of silver nano-particles (see fig. 2). The silver particles scatter the light into the Si-nc layer and thus enhance its absorption. First measurements show an enhancement of the photoluminescence of the Si-nc layer.

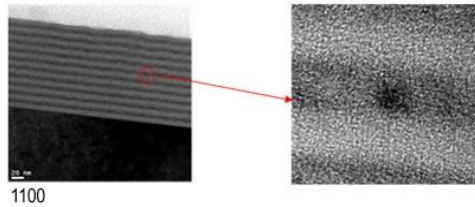


**Figure 1:** TEM image of the SRO layer hosting the Si-NCS.

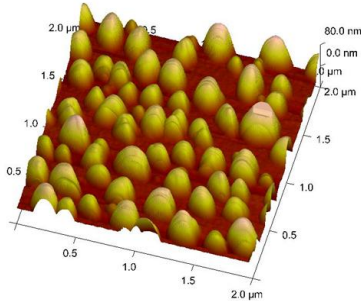


**Figure 2:** AFM image of the Ag plasmonic layer on quartz

Within the LIMA consortium (<http://www.limaproject.eu/>) we are exploring the possibility to enhance the efficiency of silicon based solar cells. We developed a prototype of a back contacted solar cell with Si-nc and silver nano-particles coating layer.

Work supported by FP7-LIMA

## 2. Silicon Nanocrystals based down shifter for enhanced silicon solar cell performance (Fabrizio Sgrignuoli)

In conventional silicon solar cell, the collection probability of photo-generated carriers shows a drop at high energy (280-400nm). One of the methods to reduce this loss is to implement nanometer sized semiconductors in solar cell where high energy photons are absorbed and low energy photons are re-emitted. This effect, called luminescence down-shifter (LDS), modifies the incident solar spectrum producing an enhancement of the energy conver-

sion efficiency of the cell. We investigate this innovative effect using silicon nanoparticles (Si-nc) dispersed in a silicon dioxide ( $\text{SiO}_2$ ) matrix (SRO). In order to reduce the optical losses of the cell, we proposed to use  $\text{SiO}_2$ /SRO double layer stack as antireflection coating (ARC) and LDS material. Optimization simulations show that controlling the different thicknesses as a function of the conversion photon probability (CE) it is possible to enhance the effect, fig 3.

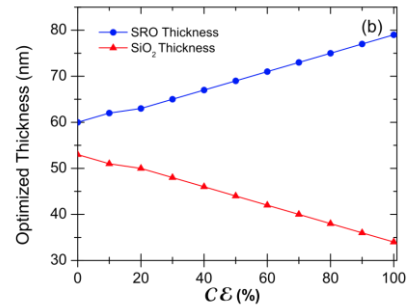


**Figure 3:** Optimized thickness combinations that maximize the short-circuit current density of a silicon solar cell as function of the conversion photon probability (CE).

These results led to investigate the CE of our device. Measured photoluminescence decay time as a function of the Si-nc local density of states yields a CE in the range 25-35% (fig. 4). Using these data, we simulated a relative improvement of 3-5 % in the energy conversion efficiency of a silicon solar cell due to the LDS effect (fig. 5). Moreover, we found a 6% relative enhancement in the energy conversion efficiency with respect to a reference silicon solar cell coated with only  $\text{SiO}_2$  as ARC.

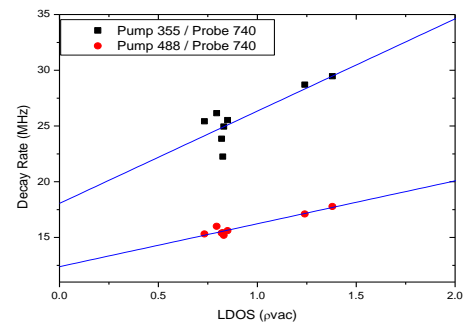


**Figure 4:** Measured PLD as a function of the local density of states for a probe 740nm wavelength.

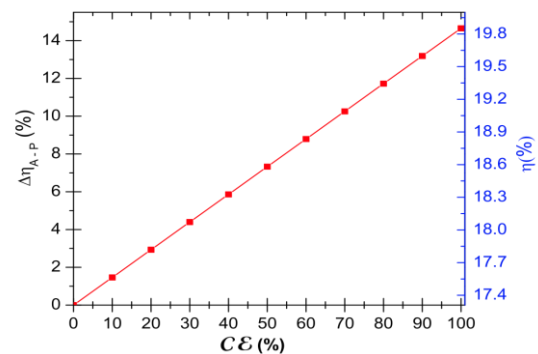


**Figure 5:** Relative enhancement in the photovoltaic conversion efficiency of a silicon solar cell due to the LDS effect as a function of the photon conversion efficiency.

Work supported by FP7-LIMA

### References:

1. Y. Jestin, G. Pucker, M. Ghulinyan, L. Ferrario, P. Bellutti, A. Picciotto, A. Collini, A. Marconi, A. Anopchenko, Z. Yuan, L. Pavesi, "Silicon solar cells with nanocrystalline silicon down shifter: experiment and modeling" Proceeding of SPIE: Next Generation (Nano) Photonic and Cell Technologies for Solar Energy Conversion, H. Loucas Tsakalakos, H. Editors, 77720B (2010).
2. Z. Yuan, G. Pucker, A. Marconi, F. Sgrignuoli, A. Anopchenko, Y. Jestin, L. Ferrario, P. Bellutti, L. Pavesi, "Silicon nanocrystals as a photoluminescence down shifter for solar cells" Sol. Energy Mater. Sol. Cells, 95, 1224 (2011).
3. F. Sgrignuoli, G. Paternoster, A. Marconi, P. Ingenhoven, A. Anopchenko, G. Pucker, L. Pavesi, J. Appl. Phys., 111, 034303 (2012)

### 3. Silicon nanocluster sensitization of erbium ions under low-energy optical excitation (Nikola Prtljaga)

The discovery of the sensitizing action of silicon nanocluster (Si-nc) on erbium ions ( $\text{Er}^{3+}$ ) offered a new material platform where silicon based optical amplifiers and laser sources could be developed. In spite of promising initial reports of optical gain and efficient electrical excitation, the demonstration of a laser action seems still to be quite challenging. While a number of limiting factors to stimulated emission has been identified, the estimates of their impact on laser action are still imprecise, partially owing to difficulties encountered when modeling the energy transfer mechanism. Although, the transfer mechanism between Si-nc and  $\text{Er}^{3+}$  has been thoroughly studied, there is no clear consensus in the literature on the more appropriate model to describe this interaction.

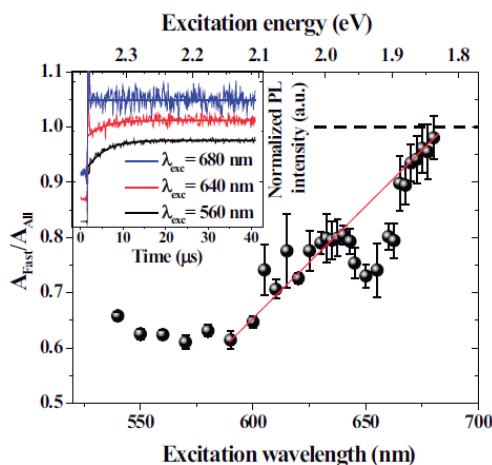


**Figure 6** Variation of the “fast” direct contribution (given by  $A_{\text{Fast}}$ , direct contribution to the first erbium excited state) to the total excited  $\text{Er}^{3+}$  population (given by  $A_{\text{All}}$ ) ratio (black spheres) with the excitation wavelength. The black dashed line represents the value at which no contribution from higher excited state of  $\text{Er}^{3+}$  ions is present. The anti-resonant feature at 650 nm is related with the direct resonant excitation of  $\text{Er}^{3+}$  ions to  $^4\text{F}_{9/2}$  energy state. The red solid line is only a guideline for the eyes. Inset: Initial PL dynamics of the  $^4\text{I}_{13/2} - ^4\text{I}_{15/2}$  transition of  $\text{Er}^{3+}$  ions under 560 nm (thin black bottom curve), 640 nm (thin red middle curve) and 680 nm (thin blue upper curve) pulsed excitation. The data have been normalized and offset by 0.2 for clarity.

Most of the studies have been performed with optical excitation in

the high energy spectral region (blue, UV) where the absorption cross section of Si-nc is dominating that of the  $\text{Er}^{3+}$  ions. Excitation at longer wavelengths (lower energies), where the absorption cross sections of these two materials become comparable, may provide a valuable insight in the energy transfer mechanism.

We demonstrate that the energy transfer to a higher energy state of  $\text{Er}^{3+}$  ions ceases to be effective for photon energies between 2.1 and 1.8 eV (0.7 - 0.55 eV of pump excess energy with respect to the energy of erbium  $^4\text{I}_{11/2}$  state). In the framework of the intra-band model, we explain this behavior in terms of the participation of sub-bandgap states in the energy transfer mechanism between Si-nc and Er. Although, we do not provide with a definitive proof of their physical nature, we correlate them with the presence of Si-nc. We confirm that the energy transfer to the first excited state of  $\text{Er}^{3+}$  remains to be the dominant excitation mechanism in the range of considered excitation energies (2.3 - 1.8 eV), implying that even with the opening of the new excitation channels, through the higher  $\text{Er}^{3+}$  excited states, only modest improvements in the efficiency of the  $\text{Er}^{3+}$  ions excitation should be expected.

### References:

1. Nikola Prtljaga, Daniel Navarro-Urrios, Alessandro Pitanti, Federico Ferrarese-Lupi, Blas Garrido, and Lorenzo Pavesi, "Silicon nanocluster sensitization of erbium ions under low-energy optical excitation", submitted to J. Appl. Phys.
2. Alessandro Pitanti, Daniel Navarro-Urrios, Nikola Prtljaga, Nicola Daldosso, Fabrice Gourbilleau, Richard Rizk, Blas Garrido, and Lorenzo Pavesi, "Energy transfer mechanism and Auger effect in  $\text{Er}^{3+}$  coupled silicon nanoparticle samples", J. Appl. Phys. 108, 053518 (2010).

### 4. Efficient infrared erbium-doped nanosilicon LEDs (Andrea Tengattini)

Silicon photonics has been proven to be a mature technology and a suitable platform for optoelectronic circuitry development. However, the monolithical integration of an efficient all silicon light source still remains to be an issue. A promising path towards light amplification in silicon is based on  $\text{Er}^{3+}$  ions sensitization by silicon nanoclusters. Erbium implanted silicon rich oxides thin film (50 nm) suitable for light emitting applications (Si-nc:Er LED) are studied by means of opto-electrical characterization. The device studied has a square gate area with a size of  $300 \mu\text{m} \times 300 \mu\text{m}$  and it is shown in the fig. 7.

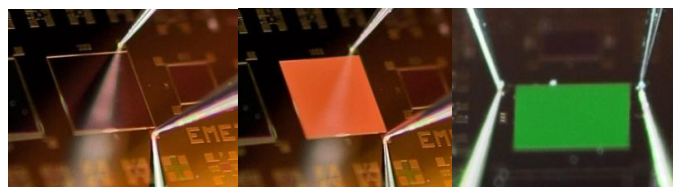


**Figure 7.** Pictures of the unbiased silicon nanocrystals (Si-NC) LED, an orange emitting Si-nc LED under forward bias and green emitting Si-nc:Er LED (from left to right).

The effect of the annealing treatments on the electroluminescence effects has been studied in detail. At the same time, light emitting diodes, based on single and multi-layer structures, with different silicon content excess, have been characterized. The maximum value of the achieved external quantum efficiency is 0.4%.

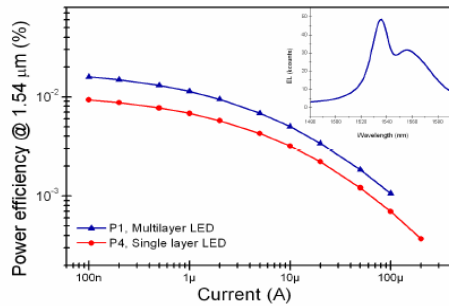


**Figure 8.** Power efficiency as a function of the injected current for a multilayer (blue) and a single layer (red) light emitting diode. The inset shows the emission spectrum in the infrared wavelength region at a fixed current equal to 1  $\mu$ A.

The multilayered structure has allowed to increase the power efficiency with respect to the single layer devices (Fig. 8). The value of the power efficiency at a fixed injected current decreases with the increase of the silicon content. Moreover, we found that both multilayer and single layer LEDs operate at high voltages, where impact excitation of Er ions and unipolar injection are the main excitation mechanisms.

The Er excitation mechanism and the electron transport in our devices change when we use bipolar pulsed electrical injection. In this case, sequential injection of electrons and holes into silicon nanoclusters takes place and non-radiative energy transfer to Er ions is observed. This mechanism occurs in a range of lower driving voltages than those observed in DC and injection frequencies higher than the Er emission rate.

Work supported by FP7-HELIOS.

#### References:

1. O. Jambois, J.M. Ramírez, Y. Berencén, D. Navarro-Urrios, A. Anopchenko, A. Marconi, N. Prtljaga, A. Tengattini, P. Pellegrino, N. Daldosso, L. Pavesi, J.-P. Colonna, J.-2. M. Fedeli, and B. Garrido. "Effect of the Annealing Treatments on the Electroluminescence Efficiency of SiO<sub>2</sub> Layers Doped with Si and Er", *J. Phys. D*, 45, 045103 (2012);
3. A. Tengattini, A. Marconi, A. Anopchenko, N. Prtljaga, L. Pavesi, J.M. Ramírez, O. Jambois, Y. Berencén, D. Navarro-Urrios, B. Garrido, F. Milesi, J.-P. Colonna, and J.-M. Fedeli. "1.54  $\mu$ m Er doped Light Emitting Devices: Role of Silicon Content", *Proceedings of the 7th IEEE International Conference on Group IV Photonics*. 2011;
4. J.M. Ramírez, F. Ferrarese Lupi, O. Jambois, Y. Berencén, D. Navarro-Urrios, A. Anopchenko, A. Marconi, N. Prtljaga, A. Tengattini, L. Pavesi, J.-P. Colonna, J.-M. Fedeli and B. Garrido. "Erbium emission in MOS light emitting devices: from energy transfer to direct impact excitation", *Nanotechnology* 23, 125203 (2012)
5. A. Anopchenko, A. Tengattini, A. Marconi, N. Prtljaga, J. M. Ramírez, O. Jambois, Y. Berencén, D. Navarro-Urrios, B. Garrido, F. Milesi, J.-P. Colonna, J.-M. Fedeli, and L. Pavesi. "Bipolar pulsed excitation of erbium-doped nanosilicon LEDs", *J. Appl. Phys.* (2012)

#### 5. Electro-optical characterization of Erbium doped slot waveguides (Davide Gandolfi)

The convergence of photonics and microelectronics within a single chip is lacking of a reliable on-chip optical amplifier. Rare-earth doped slot waveguides are thought to be a possible candidate for an on-chip amplifier. These structures increase the light confinement in the active layer and can offer the possibility of electrical injection using, for example, dielectrics embedded with silicon nanocrystals.

In our laboratories we studied slot waveguides formed by two thick silicon layers separated by a thin erbium doped silicon rich silicon oxide layer. We built a probe station for a full electro-optical waveguide characterization (fig. 9).

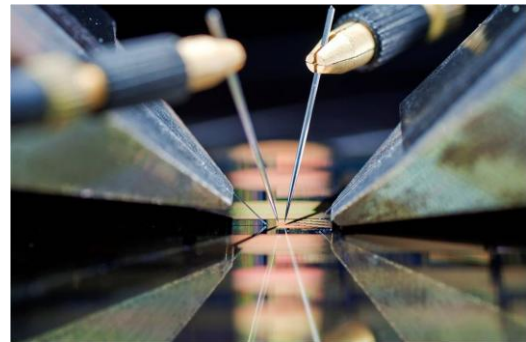


**Figure 9.** Close-up picture of the electro-optical probe station

The input and output coupling between the tapered fiber and the waveguide is performed by means of gratings (optimal incident angle 25°) written across the waveguide. With this configuration many devices can be characterized sequentially on the same wafer, increasing the testing speed.

We are able to measure optical transmission properties as a function of:

- biasing electric potential/current;
- applied electrical frequency (for AC and time-resolved measurements);
- pumping/probing light wavelength.

Moreover we can measure electrical transmission as a function of the bias voltage (I-V characteristic).

With this setup the erbium-doped slot waveguides were characterized, and showed propagation losses around 60 dB/cm at a wavelength of 1550 nm. This loss value increases with the applied voltage, due to the free-carrier absorption.

Even if this side effect prevents a working optical amplifier, we proved the presence of light emission from erbium ions by observing room temperature electroluminescence (for biasing voltages higher than 40 V) in the erbium emission band.

Further work is still required in order to engineer the energy transfer to the erbium ions without introducing unwanted losses.

Work supported by FP7-HELIOS.



## References:

1. N. Prtljaga, D. Navarro-Urrios, A. Marconi, A. Anopchenko, J.-P. Colonna, F. Milesi, N. Daldosso, O. Jambois, B. Garrido, J.-M. Fedeli, and L. Pavesi "Erbium implanted silicon rich oxide thin films suitable for slot waveguides applications", *Opt. Mater.*, 33, 1083-1085 (2011)
2. A. Tengattini, A. Marconi, N. Prtljaga, L. Pavesi, A. Anopchenko, J.-M. Fedeli, "Opto-electrical characterization of erbium-doped slot waveguides", *SPIE Photonics Europe - Conference 8431*, Bruxelles (2012)

## 6. Ensembles of Si and Ge nanostructures for photonic applications (Aleksiy Anopchenko, Alessandro Marconi)

Indirect energy gap Si and Ge nanocrystals emit light efficiently in the near-IR-visible region (fig. 10) due to quantum confinement effects when their crystalline size is smaller than the exciton Bohr radius ( $\sim 5$  nm for Si,  $\sim 24$  nm for Ge). Using size-controlled multilayer growth of Si NCs embedded in various dielectric matrices (the growth is performed at the Center for Materials and Microsystems, FBK), efficient and tunable light emission from nc ensembles is achieved. We have proposed a new scheme of light emitting diodes (LEDs) with a graded-size ensemble of Si-nc in the recombination region. Our work shows that (1) control of the tunnelling barrier and injection energy of Si-nc ensembles is possible with the size-controlled approach and (2) the graded-size Si-nc might further improve the emission properties of the LED (Fig. 10).

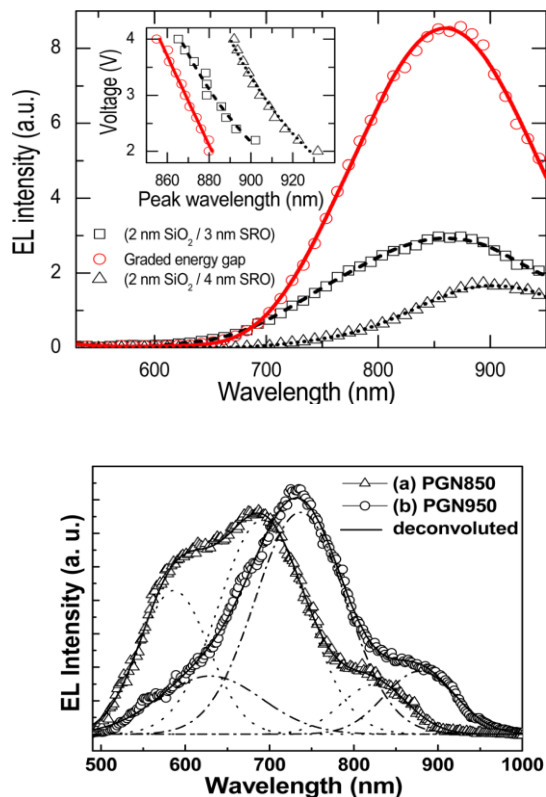


**Figure 10:** Room temperature electroluminescence (EL) of Si-nc (top) and Ge-nc (bottom) from MOS-like LEDs. Si-nc were grown using a multilayer approach. EL from two periodic and a graded multilayer Si-nc ensembles is shown on the top. Inset shows the voltage dependence of the peak wavelength.

Bottom, EL from a layer of Ge-nc with sizes 2-7 nm embedded in  $\text{Al}_2\text{O}_3$  for two Ge-nc LEDs annealed at 850 and 950 °C.

We collaborate with the IIT Kharagpur to study electroluminescence (EL) of Ge nanostructures grown by RF sputtering and pulsed laser deposition (fig. 10). In collaboration with UNSW, we have demonstrated EL from boron-doped Si nanocrystals/crystalline Si *p-n* heterojunctions. Peak emission of these boron-doped heterojunctions could be tuned from near IR (980 nm) to visible (730 nm) by an exchange of the oxide matrix, where the Si-nc are embedded in, with a nitride matrix.

We have proposed a method to measure the power efficiency of LEDs under an alternating current (AC) excitation scheme. The method is based on large-signal impedance measurements. The power efficiency of the multilayered Si-NC LEDs, which reaches 0.2 % due to direct current bipolar injection, was evaluated in AC using the proposed method. The power efficiency increases with AC driving frequency until a threshold frequency is reached, which depends on both geometry of the LED and intrinsic properties of the Si-nc ensemble, and decreases significantly for higher frequencies (fig. 11).

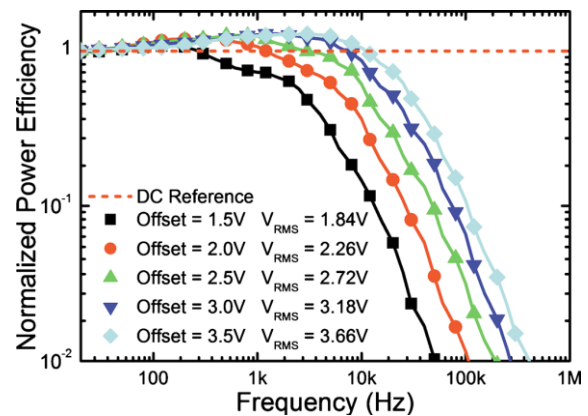


**Figure 11:** Normalized power efficiency as a function of frequency and different applied voltage bias offsets; horizontal dashed line – power efficiency level under direct current.

An optical link based on the Si-nc device operated as a bidirectional transceiver was demonstrated. The link performance was evaluated and found suitable for niche applications where the most important metrics are integrability and low cost, e.g., for lab-on-a-chip applications or for data communications in consumer electronics.

This work is supported by EC through the projects ICT-FP7-224312 HELIOS and ICT-FP7-248909 LIMA, and ITPAR-DST Nanophotonics program between the University of Trento, Italy and IIT Kharagpur, India.

## References:

1. A. Anopchenko, A. Marconi, M. Wang, G. Pucker, P. Bellutti, L. Pavesi "Graded-size Si quantum dot ensembles for efficient light-emitting diodes", *Appl. Phys. Lett.* 99, 181108 (2011).
2. S. Das, R. K. Singha, A. Dhar, S. K. Ray, A. Anopchenko, N. Daldosso, L. Pavesi "Electroluminescence and charge storage characteristics of quantum confined germanium nanocrystals", *J. Appl. Phys.* 110, 024310 (2011).
3. S. Das, S. Manna, R. Singha, A. Anopchenko, N. Daldosso, L. Pavesi, A. Dhar, S. K. Ray "Light emission and floating gate

memory characteristics of germanium nanocrystals", *Phys. Status Solidi A* 208, 635 (2011).

5. S. Manna, N. Prtljaga, S. Das, N. Daldosso, S. K. Ray, L. Pavesi "Photophysics of resonantly and non-resonantly excited erbium doped Ge nanowires", *Nanotechnology* 23, 065702 (2012).

6. D. Di, I. Perez-Wurfl, L. Wu, Y. Huang, A. Marconi, A. Tenggini, A. Anopchenko, L. Pavesi, G. Conibeer "Electroluminescence from Si nanocrystal/c-Si heterojunction light-emitting diodes", *Appl. Phys. Lett.* 99, 251113 (2011).

7. A. Marconi, A. Anopchenko, G. Pucker, L. Pavesi "Power efficiency estimation of silicon nanocrystals based light emitting device in alternating current regime", *Appl. Phys. Lett.* 98, 201103 (2011).

8. A. Marconi, A. Anopchenko, G. Pucker, L. Pavesi "Silicon nanocrystal light emitting device as a bidirectional optical transceiver", *Semicond. Sci. Technol.* 26, 095019 (2011); Cover image.

## 7. Waveguide based optical bioreactor for on-chip diagnostic (Francisco J. Aparicio Rebollo)

A large variety of biological and medical applications demand sensitive, highly specific, cost-effective, and rapid tools to analyse the concentration of specific biomolecules. Particularly the development of miniaturized devices (lab-on-chip) able to perform laboratory operations but on a small scale is very appealing for diagnostic purposes. These devices present different advantages in comparison with centralized analytical systems, mainly in situ and real time sensing. At the present optical methods represent the most widely used approach for lab-on-chip applications thanks to their high sensitivity, reliability, speed, and robustness. Specifically silicon photonics is the preferred technology for the development of sensors chips since it allows to easily integrate in the same chip (i.e. at a micrometric scale) the different optical microcomponents (waveguides, beam splitters, multiplexing systems ...) needed to confine, guide and/or process the light.

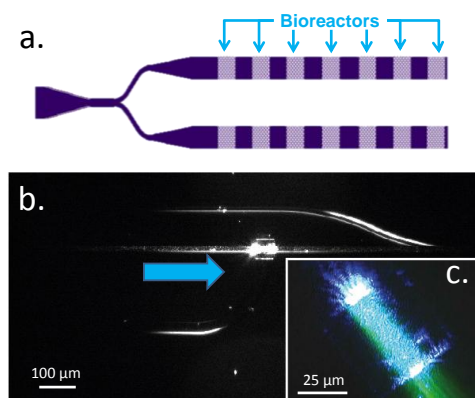


**Figure 12.** (a) Silicon photonic chip with multiple sensor sites. (b) Low magnification micrograph of a single bioreactor. Blue arrow highlights the excitation beam transmitted by the structure. (c) Fluorescence microscopy image of a bioreactor. The green light corresponds to the fluorescence emission of the infiltrated fluorophores.

Our research activity is focused on the design, fabrication and testing of a silicon waveguide-based optical sensor for proteomics.

The operation principle is based on the fluorescent detection of the proteins labeled with a luminescent marker. Thus, since the fluorescent emission can be detected with almost single-photon resolution, it is virtually possible to detect the presence of a single tagged molecule. As illustrated in Figure 12 (a) the photonic chip includes multiple bioreactors that can be selectively functionalized for the exclusively immobilization of a specific kind of protein. This strategy allows the multi-analyte detection of proteins in biological samples by using a unique chip. In these photonic structures the luminescent markers are excited by the waveguide evanescent field (see blue arrow in Figure 12 b) while the fluorescent emission (Figure 12 c) is detected by a set of SPAD photodetectors placed on top of the bioreactor where the proteins are immobilized. The evanescent field approach is chosen due to several advantages such as, among others, localized, intense and uniform illumination of the reactor site and reduction of scattered light that may hide weak fluorescence signals. Thanks to its low cost, the presented photonic chips are designed as a disposable component of a modular-stack lab-on-chip microsystem also formed by a microfluidics delivery system and a silicon SPAD detector matrix.

Work supported by FUPAT-NAOMI

## 8. Porous silicon micropowder for drug delivery (Marina Scarpa and Elena Froner)

At the end of 2011, a new project (funded by Fondazione CaRi-TRo) on the interaction of nanosystems and bio-medical field started, in collaboration with Fondazione Humanitas, in Milan. The aim of the project is to study the influence of the immune response system, in particular of macrophages, on the development of colorectal cancer (CRC) by trying to manipulate the macrophages phenotypes themselves.

The role of our laboratory is to design and set up luminescent nanoporous silicon microparticles able to deliver a specific kind of drug molecules, small interfering RNA (siRNA), to the tumor associated macrophages (TAM). When a specific siRNA enters the TAM membrane, it can lead the cell to the expression of an anti-tumoral phenotype. A drug delivery vector is required to bring the siRNA safe to the macrophages. Porous silicon microparticles are expected to be a perfect vector, as they are obtained from porous silicon disruption by sonication, they should allow high siRNA loadings inside the pores, they seem to be biocompatible (as they are degraded into silicic acid with rates depending on their chemical and morphological characteristics). Their surface can be chemically modified in order both to enhance their interaction with siRNA (inside the pores) and to stand the aggressive biological environments into which they must be delivered (with an external coating after siRNA loading). Last but not least, porous silicon microparticles (pSi MP) are luminescent and, then, no other label is needed in order to trace them in their interaction with cells or inside some model organisms.

As both the morphology (size, shape, porosity) and the surface chemistry of pSi MP are crucial for their behaviour in the body fluids and for their interaction with the TAM cells, we are now setting up both i) a protocol to select the particle sizes (and the size-families we are going to obtain will be made interact with TAM in vitro, in order to select the best one) and ii) a way to functionalize the pSi MP surfaces with different molecules (bearing reactive groups for further functionalizations) maintaining their orange-red luminescence.

Work supported by CARITRO and FUPAT-NAOMI

### 9. Optimization and synthesis of thin transparent free standing n-type porous silicon membranes (Neraji Kumar)

Since last decades, Porous silicon (PS) has been studied due to its structural and optical properties and was recognized as a potential candidate for the fabrication of highly sensitive optical sensor. Moreover fabrication of free standing membranes enables several different applications such as MEMS and sensors. For biosensing applications the porous layer should have pore sizes ranging from many tens to few hundreds of nm. In PS technology pore sizes can be partially controlled by adjusting the etching parameters (i.e. concentration of HF solution, current density, anodization time etc.). The silicon resistivity emerged as the key parameter to control pore sizes on randomly etched samples. While it is quite easy to get free standing membranes in low resistivity p-type silicon wafer; the situation is much more complex for n-type substrates. Moreover, for real applications, the membranes have to be very thin, thus high quality etching have to be engineered.

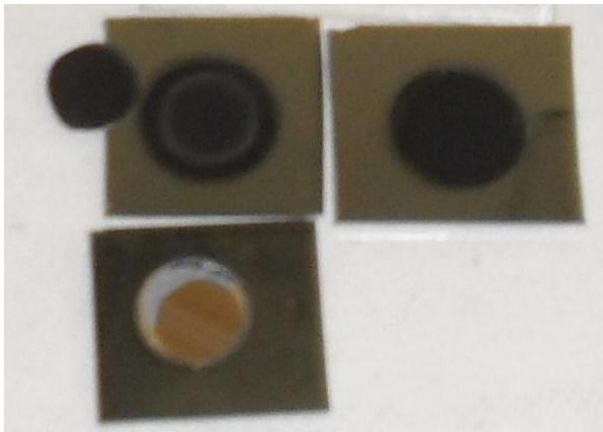


**Figure 13** Photograph of partially and completely detached n-type PSI membrane

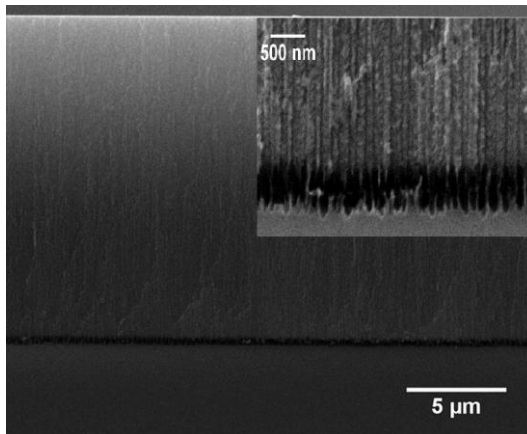


**Figure 14** SEM image of partially de-tached membrane

In this study, we investigate two types of n-type [100] silicon wafers with different resistivity: 0.1  $\Omega$ -cm and 0.01  $\Omega$ -cm. Free standing membranes composed by submicron sized pores can be prepared in medium doped n-type substrate using an optimized electrolyte solution and a “two step” etching method. As a general rules pore sizes and porosity are proportional to the concentration of water in the solution, while ethanol increases the reproducibility of the detachment of thin membranes. In low resistivity substrate (0.01  $\Omega$ cm) pore sizes can be tuned from 30 to 80 nm. Thin free standing membranes (with aspect ratio greater than 600) and pores size of 70-80 nm (porosity~60%) can be fabricated with  $H_2O$  +ethanol+  $H_2O_2$ +HF based solution using two step low current density attack. On the other side the tests performed on the higher resistivity wafers enable the fabrication of pores of few hundred nm. Because of pore sizes compatible with many biological samples, these latter structures are of great interest for bio-sensing applications and deserve a more detailed investigation.

Work supported by FP7-Positive

### References

1. J. Alvarez, P. Bettotti, I. Suarez, N. Kumar, D. Hill, V. Chirvony, L. Pavesi, J. Martinez-Pastor, Opt. Express, 19, 26106 (2011)

### 10. SCISSOR based reconfigurable optical network on chip (Mattia Mancinelli)

The bandwidth increase is currently one of the most important figure of merit to describe the innovation in network hardware. Optical networks are expanding their presence from long haul to board to board connections, thanks to the advancements of integrated silicon photonics.

In this scenario, photonic devices based on coupled optical resonators allow to use many novel effects. In particular, coupled resonators induced transparency (CRIT) effects can occur in coupled optical resonators due to classical interference. This effect was recently demonstrated in side coupled integrated spaced sequence of resonators (SCISSOR) where CRIT effect occurs when round-trip phase between 2 or many rings is an integer multiple of  $2\pi$ . If this resonant condition is satisfied, the resulting transmission spectrum exhibits very narrow transparency peak inside the resonance band of the structure (fig.15 (a)).

We develop a novel structure in order to exploit this effect and its narrow spectral linewidth. A tapered SCISSOR (TS) (fig.1(a)) is composed by a chain of N racetracks of different lengths. Each resonator differs from its neighbor by a factor  $N\Delta R$ , with  $\Delta R$  the radius difference between adjacent racetracks. N identifies the racetrack position and, in our case, ranges from  $-3$  to  $+3$ . The coupling coefficient between the waveguide and the racetracks is set by the length of the coupling section (C) and the gap between WG and resonator. L is the center-to-center distance between nearby racetracks.

Despite the use of racetracks with small radius the CRIT resonances exhibit a Q factor larger than 10000, much greater than that of a single racetrack. Moreover, this Q is obtained working in a over coupled regime with power coupling coefficient of about 40%. For this reason, TS makes the narrow linewidth immune to the mode splitting induced by roughness.



The TS has a greater flexibility than single ring designs and it can be thought as an element able to handle resonance multiplets with single channels addressing capabilities. One of these possibilities is demonstrated in Fig. 15(c) where a single channel is selected by thermal tuning of the WG sections connecting the racetracks. The physics behind this mechanism is naively sketched in fig.15(b): the large stop band sketched with a squared shape is the flat box filter resulting from the multiple resonant mechanism within the TS. We found very good agreement between experiment (fig. 15(c)) and simulations (fig 15 (d)).

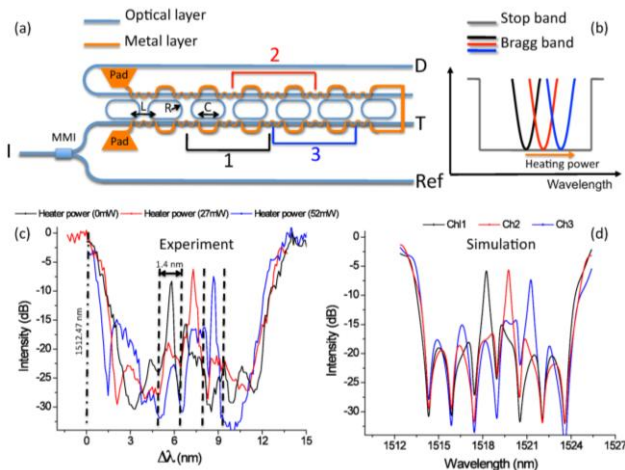


**Figure 15:** (a) Design of the SCISSOR. The optical layer is sketched in blue, while the metallic heater is in orange. (b) Schematic representation of the effect of thermal tuning on the Bragg band. (c) Experimental transmission spectrum of the T port for different heater powers: (black) 0 mW, (red) 27 mW, (blue) 52 mW. The dashed lines delimit the widths of the CRIT channels. (d) Theoretical transmission spectrum of the T port. All the data are normalized to the Ref port.

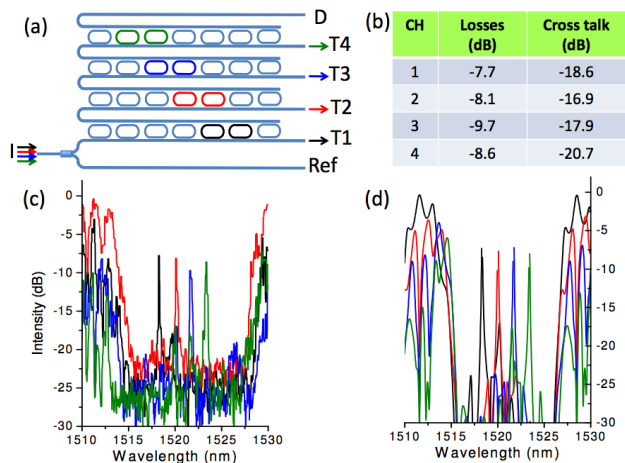


**Figure 16:** Scheme of  $1 \times 4$  mux/demux and its trasmission spectra. (a) Sketch of the multiplexer composed by 4 TS with different active channels (black, red, blue, green). (b) values of channel losses and crosstalk. (c) Experimental transmission spectra for the ports T1-4; (d) theoretical spectra of the four T ports.

Each channel can be also independently switched on/off using a local refractive index changes. The effect of this perturbation is to annul the radius difference  $\Delta R$  within the active racetrack pair. Therefore, the CRIT condition is broken and the resonance suppressed. We got an amplitude extinction ratio of about 10 dB for the channel 1. The -12 dB of cross talk remains unchanged by the switching process. The dynamic switching reveals also that the

commutation speed is faster than 130 ps (our electronic bandwidth).

Fig. 16(a) shows the scheme of a  $1 \times 4$  mux/demux. This structure consists of a combination of 4 TS in cascade where the input of a TS is the D port of the previous one. Each TS is designed to transmit different CRIT channels, by a proper selection of L (different L means different Bragg band position). Since the 4 TS differ only by their L and this variation accounts only for a 0.15% among the four different SCISSOR, the stop band edges remain unaffected. When the input signal that enters in the structure has a wavelength inside the stop band but different from those of CH1-4, it crosses all the SCISSORS and exits through port D. On the other hand, wavelengths resonant with CH1-4 are routed in different output waveguides (T1-4). Obviously the same structure works as a multiplexer if the inputs are mirrored. Fig. 16(c) reports the experimental spectra obtained without any thermal tuning on the multiplexer. Panel (d) shows the simulated spectra. These data confirm the device robustness versus fabrication errors. Furthermore this high reliability in device fabrication will enable a sensible decrease of power consumption required to tune the device to its working wavelength and to keep it in its operational state. Channel losses and cross talk for each CRIT channel are shown in Fig. 16(b).

TS is an innovative optical switch with important advantages if compared with other optical schemes:

- the use of coupled resonators allows the achievement of very high Q- factor, using low Q resonators;
- the high coupling regime of operation keeps insertion losses to very low values without degrading CRIT Q factor;
- CRIT resonances do not shift during the switching process and remain fixed within their own channel space.

#### References:

1. P. Bettotti, M. Mancinelli, R. Guider, M. Masi, M. Rao Vana-charla, and L. Pavesi "Robust design of an optical router based on a tapered side-coupled integrated spaced sequence of optical resonators", *Optics Letters*, Vol. 36, Issue 8, pp. 1473-1475 (2011)
2. M. Mancinelli, R. Guider, P. Bettotti, M. Masi, M. R. Vana-charla, and L. Pavesi "Coupled-resonator-induced-transparency concept for wavelength routing applications", *Optics Express*, Vol. 19, Issue 13, pp. 12227-12240 (2011).

#### 11. Porous silicon biosensing (Paolo Bettotti)

Food allergies are common in 1-2% of adults and up to 8% of children, corresponding to a serious public health problem that affects over 15 million people in Europe from infants to the elderly and its prevalence is increasing. In searching for alternative point of care techniques, recent advances in the optics/photonics industries have permitted significant development activity for smart biosensor systems. The interest stems from their intrinsically high sensitivities and compatibility with mature silicon microchip processing that permit mass production and integration of high-throughput arrays of compact devices on a single-chip for simultaneous detection of several analytes and, as such, inexpensive, easy to use and portable smart sensors.



Porous silicon (PS) is an almost ideal material as a signal transducer for label free optical biological sensing with many advantages, which include: (1) ease of fabrication (by the electrochemical etching of a silicon wafer in hydrofluoric acid) of high-quality optical elements with a nanoporous sponge-like structure, (2) the possibility of integration with wafer level IC processing, (3) an extremely large internal surface ( $\sim 500 \text{ m}^2/\text{cm}^3$ ) that can in principle be leveraged to enhance device sensitivity many orders of magnitude over a planar device of comparable transducer diameter, (4) tuneable pore sizes across biologically relevant length scales, (5) convenient covalent and non-covalent surface chemistry.

The PS birefringent properties were characterized for a set of samples consisting of nanoporous silicon etched into p-type (110) Si with resistivity of 0.01-0.001 Ohm/cm. Pores sizes were in the range of few tens of nanometers. Birefringence and sensitivity of anisotropic porous silicon membranes were characterized optically in collaboration with the UMDO, Materials Science Institute, University of Valencia, demonstrating a record sensitivity of 1245 nm/RIU at 1500 nm.

Furthermore a proper stabilization of the surface structure was achieved by using a mild thermal oxidation and we demonstrate that oxidized porous silicon membranes have optical parameters with long term stability.

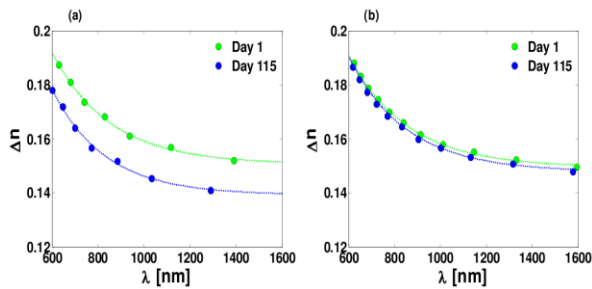


**Figure 17** Birefringence of porous silicon free standing membranes. Green data refers to samples measured soonly after fabrication, while blue data are for samples stored in ambient air for four months. (a) Measurements for non passivated samples, (b) measurements for annealed sample.

Work supported by FP7-Positive

#### References:

1. J. Alvarez, P. Bettotti, I. Suarez, N. Kumar, D. Hill, V. Chirvony, L. Pavesi, J. Martinez-Pastor "Birefringent porous silicon membranes for optical sensing", Opt. Express, 19, 26106 (2011)

## 12. Two-dimensional micro-Raman mapping of stress and strain distributions in strained silicon waveguides (Federica Bianco)

Thanks to the strain dependence of the opto-electronic properties of silicon, strain engineering of silicon-on-insulator (SOI) structures is often used to improve the existing functionalities or to enable novel ones. Particularly, strained silicon is currently emerging as new material for photonic devices with applications both in signal modulation and in nonlinear optical wavelength generation. Consequently, these new sophisticated structures require a careful stress engineering and the study of strain distribution before full device fabrication.

With this purpose, the micro-Raman spectroscopy is efficiently employed as a non-destructive technique allowing to measure mechanical stress with micrometric spatial resolution. Basically, the Raman scattered phonon wavenumber in strained condition is shifted from the value in unstrained condition and the amount of the shift is strictly related to the magnitude and direction of the applied stress.

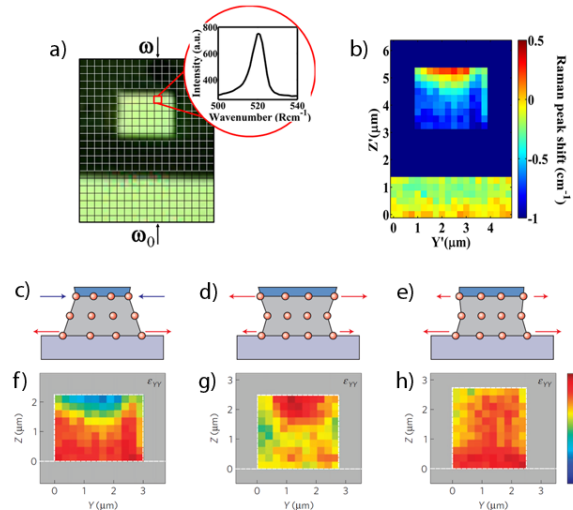


**Figure 18:** Strain characterization: a) scanning grid (not to scale) over imposed to an optical image of the waveguide facet. The inset shows a typical Raman spectrum. The two arrows point to the measured Raman frequency in the strained silicon ( $\omega$ ) and the measured Raman frequency in the unstrained bulk silicon ( $\omega_0$ ); b) map of the Raman peak shift,  $\Delta\omega_{\text{obs}} = \omega - \omega_0$ ; c-e) Schematic representations of the SOI1, 2, 3 waveguides. The arrows indicate the observed effect of the stressing overlayer (blue layer), which can be tensile or compressive-like. The deformation effect is exaggerated; f-h) Two-dimensional maps of the strain tensor component  $\epsilon_{yy}$  for the SOI1, 2, 3  $2 \mu\text{m}$ -wide waveguides.

By scanning the facet of strained SOI waveguide (fig. 18(a)) and estimating the Raman peak shift for each probed region (fig. 18(b)), we built a two dimensional strain distribution map as a function of the applied stress. An overlayer is used to exert the stress. By changing the deposition parameters of the overlayer, a compressed sample (called SOI1), a stretched sample (called SOI2) and stress-compensated sample (called SOI3) were fabricated and the resulting deformation sketches are shown in Fig. 18 (c), 18 (d), 18 (e).

As can be seen in Fig. 18 (f), 18 (g), 18 (h), the two dimensional distribution of the strain tensor component  $\epsilon_{yy}$  for the sample SOI1, 2, 3, respectively, has a strong inhomogeneity, whose degree is mainly determined by the action of the stressing overlayer, which combines with the always-compressive contribution of the underlying buried oxide.

With these results we demonstrated the presence of a high crystalline deformation into the waveguides and thus the breaking of the silicon centrosymmetry, which enables the second order nonlinear susceptibility.

Work supported by FUPAT NAOMI and CARIPLO

#### References

1. F. Bianco, K. Fedus, F. Enrichi, R. Pierobon, M. Cazzanelli, M. Ghulinyan, G. Pucker, L. Pavesi, "Two-dimensional micro-

Raman mapping of stress and strain distributions in strained silicon waveguides”, in preparation.

2. M. Cazzanelli, F. Bianco, E. Borga, G. Pucker, M. Ghulinyan, E. Degoli, E. Luppi, V. Vénier, S. Ossicini, D. Modotto, S. Wabnitz, R. Pierobon & L. Pavesi, “Second-harmonic generation in silicon waveguides strained by silicon nitride”, *Nature Materials* **11** 148-154 (2012)

Work supported by FUPAT NAOMI and CARIPLO

### 13. Second-harmonic generation in silicon waveguides strained by silicon nitride (Massimo Cazzanelli)

Nonlinear silicon photonics is a novel research field that enables the realization of novel photonic devices. Most of the reported results have exploited the well-known third-order nonlinear susceptibility of silicon. A much more efficient way to convert light in silicon devices would rely on second-order effects (i.e.  $\chi^{(2)}$ ), but the crystalline centro-symmetry of silicon prohibits these possibilities. Our idea is to inhomogeneously break the crystalline symmetry of silicon via mechanical strain and induce a non-zero second-order susceptibility for nonlinear optical wavelength conversion into silicon waveguides.

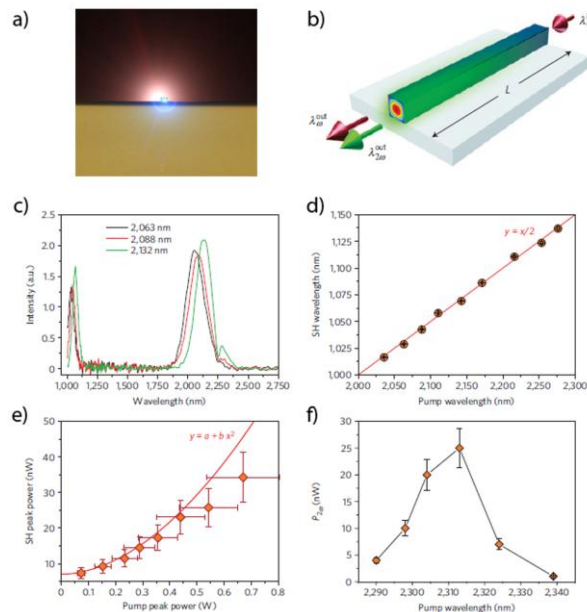


**Figure 19:** a): Artistic image of second-harmonic generation in a silicon waveguide (© Mher Ghulinyan). b): the second-harmonic experiment, where  $L$  is the total waveguide length. A train of pulses are coupled into the waveguide at a wavelength  $\lambda_0$ , and two signals (at wavelengths  $\lambda_0$  and  $\lambda_{20}$ ) are measured at the output of the waveguide. c): Waveguide transmission spectra. In addition to the transmitted pump signal at about 2100 nm, a SH signal is recorded at about 1050 nm. d) SH peak tunability curve. The linear shift of SH peak with the pump wavelength spans over 300 nm of variation of the pump wavelength. e) Peak power dependence of the second-harmonic signal. As theoretically expected, the SH power quadratically changes with the pump power. f) Dependence of the SH peak power  $P_{20}$  on the pump wavelength  $\lambda_0$ .

To explore this concept, we carried out second-harmonic-generation experiments (fig. 19 (b)) by using inhomogeneously strained Si waveguides obtained by deposition of stressing  $\text{SiN}_x$

claddings. From the measured efficiencies  $\eta$  we estimated a  $\chi^{(2)}$  of several tens of pm/V, which represents a very large value, much higher than the usually reported values due to surface effects. Moreover, by comparing different samples,  $\chi^{(2)}$  shows a trend related to the inhomogeneity and magnitude of the strain. In particular, the higher is the deformation the stronger is the induced- $\chi^{(2)}$ . These experimental results were also confirmed by ab-initio calculations (performed by the Nanostructure Modeling Group, University of Modena e Reggio Emilia), which simulate the second-order nonlinear optical response from strained bulk Si by moving the Si atoms in the lattice.

Because of the sizeable values and the observed dependence of  $\chi^{(2)}$  on the stressing layer and, in particular, on the strain inhomogeneity, we believe that such a second-order susceptibility has a bulk origin. Consequently, this represents the first experimental observation of second harmonic generated inside silicon waveguides.

Work supported by FUPAT NAOMI and CARIPLO

### References

1. M. Cazzanelli, F. Bianco, E. Borga, G. Pucker, M. Ghulinyan, E. Degoli, E. Luppi, V. Vénier, S. Ossicini, D. Modotto, S. Wabnitz, R. Pierobon & L. Pavesi, “Second-harmonic generation in silicon waveguides strained by silicon nitride”, *Nature Materials* **11** 148-154 (2012)

### 14. Monolithic Whispering-Gallery Mode Resonators With Vertically Coupled Integrated Bus Waveguides (Fernando Ramiro Manzano)

One of the most interesting fields in photonics is the light confinement in a cavity. Light energy stored in a small volume increases dramatically the interaction with matter, thus allowing the development of devices with improved properties.

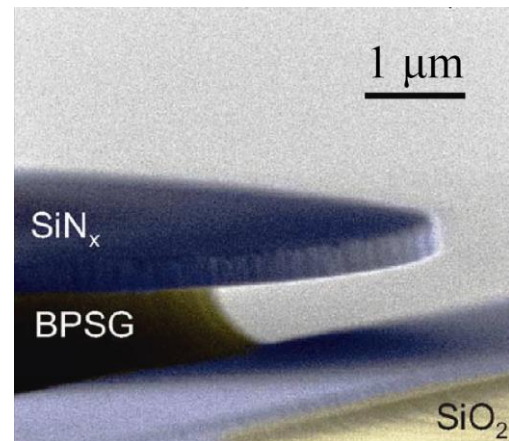


**Figure 20** Coloured SEM image of a whispering-gallery mode resonator with vertically coupled integrated bus waveguide. (© Mher Ghulinyan)

Technological advances in lithography techniques in circular based cavities, so called planar whispering gallery mode (WGM) resonators, have enabled the development of a quasi-free-standing cavity embedded in air environment. This configuration has improved drastically one of the most important requirements for a WGM resonator: the refractive index contrast. Most of current

cutting-edge experiments with this kind of devices regularly use tapered fibers to probe the system. In this scheme, a tapered fiber is laterally approached to the cavity to a distance that allows an evanescent field coupling. Positioning the tapered fiber requires the use of piezoelectric controllers to provide nanometric coupling gap. This, however, results in unstable experimental conditions.

We have developed a silicon-based microresonator/waveguide coupled system, fully integrated on a silicon chip. The device uses a vertical coupling scheme of the resonator and a buried strip waveguide (fig. 20). The high optical quality of the device follows from the accurate planarization of the waveguide topography, which is achieved by multiple depositions and reflows of a borophosphosilicate glass over strip waveguides. In addition, the vertical coupling allows nanometric control of the coupling gap without the need to use ultrahigh resolution lithography, such as deep-UV or electron beam lithography.

This monolithic configuration enables the wafer-scale mass fabrication of freestanding planar resonators suspended in air and coupled to integrated bus waveguides. It opens the door for the realization of stable all-integrated complex resonator systems for optomechanical and metrological applications, with the potential to substitute today's intensive use of complicated fiber-taper coupling schemes.

Work supported by FP7-Appcoptor

#### **For more info**

Nanoscience Laboratory  
Physics Department - Science Faculty  
University of Trento  
via Sommarive 14  
38123 Povo- Trento (Italy)  
<http://www.unitn.it/en/dphys/7421/nanoscience>  
<http://science.unitn.it/~semicon/>

secretary dott. Tatsiana Yatskevich  
email [tanya@science.unitn.it](mailto:tanya@science.unitn.it)  
phone +390 461 283172  
fax +390 461 282967